HHS Public Access

Author manuscript

J Immunol. Author manuscript; available in PMC 2016 August 15.

Published in final edited form as:

J Immunol. 2015 August 15; 195(4): 1417–1426. doi:10.4049/jimmunol.1402708.

Circulating human CD27-IgA+ memory-B cells recognize bacteria with polyreactive immunoglobulins[1]

Magdalena A. Berkowska[*,§], **Jean-Nicolas Schickel**[†], **Christina Grosserichter-Wagener**[*], **Dick de Ridder**[‡,¶], **Yen Shing Ng**[†], **Jacques J.M. van Dongen**[*], **Eric Meffre**[†,‖], and **Menno C. van Zelm**[*,‖]

[*]Dept. Immunology, Erasmus MC, University Medical Center, Rotterdam, the Netherlands. [†]Dept. Immunobiology, Yale University School of Medicine, New Haven, Connecticut, USA. [‡]The Delft Bioinformatics Lab, Faculty of Electrical Engineering, Mathematics and Computer Science, Delft University of Technology, Delft, The Netherlands.

Abstract

The vast majority of immunoglobulin (Ig)A production occurs in mucosal tissue following T-cell dependent and T-cell independent antigen responses. To study the nature of each of these responses, we analyzed the gene expression and Ig reactivity profiles of T-cell dependent CD27+IgA+ and T-cell independent CD27−IgA+ circulating memory-B cells. Gene expression profiles of IgA+ subsets were highly similar to each other and to IgG+ memory-B-cell subsets with typical upregulation of activation markers and downregulation of inhibitory receptors. However, we identified the mucosa-associated *CCR9* and *RUNX2* genes to be specifically upregulated in CD27−IgA+ B cells. We also found that CD27−IgA+ B cells expressed antibodies with distinct Ig repertoire and reactivity than those from CD27+IgA+ B cells. Indeed, antibodies from CD27−IgA+ B cells were weakly mutated, often utilized Igλ chain and were enriched in polyreactive clones recognizing various bacterial species. Hence, T-cell independent IgA responses are likely involved in the maintenance of gut homeostasis through the production of polyreactive mutated IgA antibodies with crossreactive anti-commensal reactivity.

[1]This work was supported by a Fellowship from the Ter Meulen Fund – Royal Netherlands Academy of Sciences to M.A.B., Fellowships from the Erasmus University Rotterdam and Erasmus MC to M.C.v.Z. and grant numbers AI071087, AI082713, AI095848 and AI061093 from NIH-NIAID to E.M.

Correspondence: Dr. Menno C. van Zelm, Department of Immunology, Unit Molecular Immunology, Erasmus MC, University Medical Center, Wytemaweg 80, 3015 CN Rotterdam, The Netherlands, Phone: +31-10-7043038, Fax: +31-10-7044731, m.vanzelm@erasmusmc.nl, Dr. Eric Meffre, Department of Immunobiology, Yale University School of Medicine, 300 George Street, New Haven, CT 06511, USA, Phone : +1-203-737-4535, Fax : +1-203-737-2704, eric.meffre@yale.edu.
[§]Current address: Dept. Experimental Immunohematology, Sanquin Research and Landsteiner Laboratory, Amsterdam, The Netherlands.
[¶]Current address: Bioinformatics Group, Wageningen University, Wageningen, The Netherlands
[‖]E.M. and M.C.v.Z. are joint senior authors of this study.

Disclosures

The authors declared no competing interests.

Introduction

The microbiome of the human gastrointestinal tract contains large numbers of bacteria of up to 30,000 different species (1). The majority of these bacteria are coated with immunoglobulins (Ig) (2) that are generated in dynamic responses (3, 4). Indeed, the mucosal surfaces of the intestinal tract, the oral cavity and lungs are major sites of antibody production, mainly the secretory form of IgA (5).

Each B cell carries surface Ig generated through V(D)J recombination of Ig heavy (IgH), and Igκ and Igλ light chain genes during stepwise differentiation in the bone marrow (6, 7). Upon antigen recognition, these newly generated B cells undergo responses involving affinity maturation by induction of somatic hypermutations (SHM) in the Ig variable domains and class-switch recombination (CSR) from the IgM to e.g. the IgA isotype (8). SHM and CSR are mediated by activation-induced cytidine deaminase (AID) (9), which is upregulated through CD40 signaling following interaction with CD40L on activated CD4+ T cells. Such T-cell dependent (TD) responses take place in germinal center reactions in lymphoid tissues. Alternatively, AID expression can be induced in T-cell independent (TI) B-cell responses, which are associated with limited proliferation and affinity maturation to lipid or carbohydrate structures (8, 10–13). TI class-switching towards IgA is well-supported by the microenvironment of the gut, especially by dendritic cells (DC) in the gut-associated lymphoid tissue. These DCs secrete retinoic acid (RA) that activates circulating B cells to induce expression of adhesion molecule α4β7 and chemokine receptor CCR9, which mediate gut homing (14). Upon activation via Toll-like receptors (TLR), DCs and monocytes secrete BAFF and APRIL, which bind TACI on B cells and can induce CD40-independent class-switching towards IgA (15–18). In addition, DC-derived TGFβ and RA act in concert with IL-5, IL-6 and IL-10 to induce differentiation of B cells into antibody secreting plasma cells (14, 18–20).

Although about 25% of intestinal IgA-producing plasmablasts are polyreactive, they show molecular signs of antigen-mediated selection (21), fitting with antigen-induced production rather than secretion of “natural antibodies” independent of antigen stimulation. It is tempting to speculate that TI IgA is directed against cell-wall components of commensal bacteria to support the formation of a biofilm and to disable their translocation through the epithelial layer (22, 23). This would prevent priming of systemic high-affinity TD responses to beneficial gut microbiota. Indeed, MyD88/TRIF double-knock-out mice deficient in TI IgA production spontaneously developed systemic responses against gut microbiota (24).

We recently distinguished two circulating human IgA+ memory-B-cell subsets: conventional CD27+IgA+ cells were dependent on T-cell help, whereas unconventional CD27−IgA+ cells were present in CD40L-deficient individuals (25). Moreover, the limited replication history of CD27−IgA+ memory-B cells, their low frequency of SHM and increased IgA2 usage were features reminiscent of IgA+ B cells from the intestinal *lamina propria* (25, 26). We show here that both CD27+IgA+ and CD27−IgA+ B-cell subsets are typical memory-B cells as evident from their gene expression profiles and detailed immunophenotypes. From single cell-sorted CD27+IgA+ and CD27−IgA+ memory-B cells we produced *in vitro* recombinant antibodies to assess their reactivity to various antigens

and bacterial strains. We found that a large fraction of CD27−IgA+ memory-B cells express polyreactive antibodies with a unique repertoire and reactivity towards commensal bacteria, suggesting that these B cells play an important role in maintaining mucosal immunity.

Materials and Methods

Cell sorting and gene expression profiling

Three naive and six human memory-B-cell subsets were purified from post-Ficoll mononuclear cells on a FACSAriaI cell sorter (BD Biosciences) (25, 27). Naive B cells were separated into CD38+CD27−IgD+IgM+ transitional B cells, $CD38^{dim}$CD27−IgD+IgM+CD5+ pre-naive B cells and $CD38^{dim}$CD27−IgD+IgM+CD5− mature naive B cells, and memory B cells into $CD38^{dim}$CD27−IgD+IgM+ natural effector B cells, $CD38^{dim}$CD27−IgD−IgM+ 'IgM-only' B cells, $CD38^{dim}$CD27+IgA+, $CD38^{dim}$CD27+IgG+, $CD38^{dim}$CD27− IgA+ and $CD38^{dim}$CD27−IgG+ subsets. RNA was isolated from each sorted subset with the RNeasy Mini Kit (Qiagen). Gene expression was quantified using Affymetrix HG-U133 Plus 2.0 GeneChip arrays (containing 54,675 probe sets), as previously described (7, 27, 28), and all data have been deposited in ArrayExpress (http://www.ebi.ac.uk/arrayexpress/; accession numbers E-MEXP-3767 and E-MTAB-3637). Expression profiles of the three naive and six memory-B-cell subsets from 3 healthy donors were compared based on the perfect match probe intensity levels. RMA background removal and quantile normalization were performed, followed by a per-probe set two-way ANOVA (with factors probe and cell type). This resulted in average expression levels for each probe set in each cell type, as well as *p* values for the significance of the difference between cell types. The *p* values were adjusted for multiple testing using Šidák stepdown adjustment (29), and all differences with adjusted *p* values <0.05 were considered significant.

The maximum absolute difference in expression between any two cell types was calculated to select probe sets that showed a signal. Only probe sets that showed larger differences than a $\log_2$ threshold value of 0.7 were selected for clustering. Correlation ρ between samples was then calculated based on only these selected probe sets, and the data was hierarchically clustered (complete linkage) using $1-\rho$ as a distance measure (28).

Single-cell sorting

Post-Ficoll mononuclear cells from healthy donors were enriched for B cells by magnetic separation with CD19 or CD20 microbeads (Miltenyi Biotech) and stained with CD20-PE-Cy7, CD27-APC (both from Biolegend), CD38-FITC (BD Pharmingen), CD27-APC and IgA-PE (Southern Biotech) prior to purification. Single CD20+$CD38^{dim}$CD27+IgA+ and CD20+$CD38^{dim}$CD27−IgA+ memory-B cells were sorted on a FACSAria flow cytometer (BD Biosciences) into 96-well PCR plates and immediately frozen on dry ice.

cDNA synthesis, Ig genes amplification, antibody production, and purification

RNA from single cells was reverse-transcribed in the original 96-well plate in 12.5-μl reactions containing 100 U Superscript II RT (Life Technologies) for 45 minutes at 42°C. RT-PCR reactions and primer sequences were as described previously (30–32), suplemented with an *IGHA*-specific primer (5'-CTTTCGCTCCAGGTCACACTGAG-3') for the 1st PCR

reaction. Cloning strategy, expression vectors, antibody expression, and purification were performed as described previously (30, 31), Ig sequences were analyzed by IgBLAST comparison with GenBank. IgH-CDR3 was defined as the interval between the conserved arginine/lysine at position 94 in IGHV-FR3 and the conserved tryptophan at position 103 in the *IGHJ* gene. SHM selection strengths were determined using the BASELINe program (http://selection.med.yale.edu/baseline/).(33)

ELISAs and immunofluorescence assays

Antibody reactivity analysis was performed as described previously with the highly polyreactive ED45 antibody as positive control for HEp-2 reactivity and polyreactivity (30, 31). Antibodies were considered polyreactive when they recognized the 3 distinct antigens: dsDNA, insulin, and LPS. ELISA plates for bacteria-reactivity testing were coated with purified flagellin from *B. subtilis* (InvivoGen), or sonicated lysates from cultured *E. cloacae* (ATCC 13047), *E. faecalis* (ATCC 29212), *E. coli* or *S. aureus*, or obtained by multiple cycles of freezing and thawing lysates from *B. fragilis* (ATCC 2528), and *C. difficile* (ATCC 9689) at a concentration of 1 ng/μl. For indirect immunofluorescence assays, HEp-2 cell-coated slides (Bion Enterprises Ltd.) were incubated in a moist chamber at room temperature with purified recombinant antibodies at 50–100 μg/ml according to the manufacturer's instructions. FITC-conjugated goat anti-human IgG was used as detection reagent.

Statistical analysis

Statistical analyses were performed with the two-tailed Student's *t* test, Mann-Whitney *U* test, or χ^2 test as indicated in details in the Figure legends. *P* values < .05 were considered statistically significant.

Results

Gene expression profiling of naive and memory-B-cell subsets

Circulating CD27+IgA+ and CD27−IgA+ B cells both display a memory-B-cell phenotype with distinct features, suggesting that they may originate from different types of immune responses (25). To study whether the TI origin of CD27−IgA+ B cells results in a typical memory-B-cell transcription program, we compared their gene expression profile with 3 naive and 5 other memory-B-cell subsets.

Unsupervised clustering analysis based on 399 probe sets that showed the greatest variation in expression between any two samples yielded three main clusters (Fig. 1A). Cluster 1 comprised the three naive-B cells (transitional, pre-naive and mature naive), cluster 2 the natural effector and IgM-only memory-B cells, and cluster 3 the Ig class-switched CD27+IgA+, CD27+IgG+, CD27−IgA+ and CD27−IgG+ memory-B cells (Fig. 1A). Among class-switched memory-B cells, CD27+IgA+ cells mostly resembled CD27+IgG+ cells, and CD27−IgA+ cells were most similar to CD27−IgG+ cells (Fig. 1A). The expression patterns of these 399 probe sets in CD27−IgA+ B cells correlated well with all Ig-class switched cells, showed medium correlation with the IgM+ memory-B-cell subsets and differed mostly from naive-B cells (Fig. 1B, Supplemental Table I).

All 9 B-cell subsets showed high gene expression levels of pan-B markers CD19, CD20, BAFF-R, CD79A and CD79B (Fig. 1C, Supplemental Table I), and the gene expression levels for markers that were used to define the subsets (CD5, CD38, IgM, IgD, IgA, IgG, CD27) correlated well with their protein expression levels. In addition, all memory-B-cell subsets showed the expected increase in activation markers and co-stimulatory molecules, such as CD80, CD86, TACI, FAS and CD58, and downregulation of genes encoding inhibitory receptors CD22 and CD72 as compared to naive-B-cell subsets (Fig. 1C) (25, 34). These expression patterns were confirmed at the protein level by flow cytometry (Fig. 2A) (25). *TLR* gene expression levels were similar for IgA+ and other memory-B cells (Supplemental Table I), although CD27−IgA+ cells contained fewer *TLR1* and more *TLR10* transcripts than mature naive-B cells. However, membrane TLR-1 and TLR-10 expression levels were similarly low in naive and memory-B-cell subsets (Fig. 2A). In addition, there were no signs of TLR-signaling pathway deregulation in IgA+ cells. Furthermore, CD27−IgA+ memory B cells showed similar expression of signaling molecules involved in BCR and CD40-signaling pathways to all other memory B-cell subsets. Comparison with mature naive B cells revealed upregulation of *GAB2, GRB2* (adaptor molecules in the BCR-signaling pathway) and downregulation of *LYN* in CD27−IgA+ B cells, as well as downregulation of *TANK* in CD40-signaling pathway. However, the majority of transcripts from both signaling pathways were not expressed significantly different between the subsets. Both IgA+ B-cell subsets showed low *IL4R* and high *IL6R* and *IL10RA* expression, supporting the role of IL-6 and IL-10 in IgA+ memory-B-cell differentiation (Supplemental Table I).

The Runx2 and Runx3 transcription factors act downstream of TGF-β and retinoic acid (RA) signaling pathways to induce TI class-switching towards IgA in the gut (35). While *RUNX3, TGFBR* and *RARA* transcript levels were similarly high in all analyzed B-cell subsets, *RUNX2* was exclusively expressed by IgA+ B cells (Fig. 1, Fig. 2B, Supplemental Table I), especially in CD27−IgA+ B cells, supporting their TI origin. Thus, CD27−IgA+ B cells appear to be true memory-B cells; they display the highest expression of *RUNX2*, which may play an important role in their development.

Differential expression of mucosa homing-related genes by B-cell subsets

Expression of chemokine receptors on lymphocytes determines their ability to migrate in response to stimuli. All analyzed B-cell subsets expressed lymph node homing receptors *CXCR4* and *CCR7*, but their levels were significantly higher on naive than on class-switched memory-B cells (Supplemental Table I). CCR7 protein was present on nearly all mature naive-B cells, but only on a fraction of cells within each memory-B-cell subset (Fig. 2A).

Stimulation of chemokine receptors induces surface expression of diverse adhesion molecules. All B-cell subsets showed similarly high expression of genes encoding CD62L (*SELL*), $\alpha_4\beta_7$ (*ITGA4/ITGB7*), and LFA-1 (*ITGAL/ITGB2*) involved in migration to lymph nodes (36, 37). In addition, *ITGB1*, which encodes the β1 subunit of the $\alpha_4\beta_1$ integrin, was upregulated in all memory-B cells (Supplemental Table I). Although none of the B-cell subsets expressed the mucosal homing marker *CCR10* (38), CD27−IgA+ B cells specifically expressed the small-intestine homing receptor *CCR9* (Supplemental Table I) (39).

Membrane CCR9 protein expression was only detectable on a fraction of cells within this B-cell subset (7.9% of CD27−IgA+ memory B cells; Fig. 2A). We conclude that CD27−IgA+ B cells contain clones with the capacity to home to the intestinal tract.

Distinct Ig gene repertoires in CD27+IgA+ and CD27−IgA+ B cells

The distinct maturation pathways of CD27+IgA+ and CD27−IgA+ memory-B cells were hardly reflected in their transcription program. However, previous observations indicated that these two IgA+ memory-B-cell subsets harbored distinct Ig repertoires (25). To study the Ig repertoire and reactivity of CD27+IgA+ and CD27−IgA+ memory-B cells, we single-cell purified these from the blood of 5 healthy donors.

The *IGHV* subgroup and *IGHJ* gene distributions in CD27+IgA+ and CD27−IgA+ memory-B cells were similar to each other (Fig. 3A, Supplemental Table II) (40), and to previously reported naive-B cells (30). More than half of the cells utilized a member of the large *IGHV3* subgroup, followed by *IGHV4* (~16%) and *IGHV1* (~10% in CD27+IgA+, and ~20% in CD27−IgA+ B cells). In both subsets, *IGHV3-23*, *IGHV3-30*, *IGHV3-33* were the most frequent *IGHV3* genes, and *IGHV4-59* was the most frequent *IGHV4* gene. *IGHJ4* was the most often used *IGHJ* gene, followed by *IGHJ5* and *IGHJ6*. The IgH-CDR3 regions in rearrangements from both IgA+ subsets showed similar length distributions with the majority of regions 10–14 amino acids in size and did not differ in the content of positively charged amino acids (arginine, lysine and histidine) (Fig. 3B). CD27−IgA+ B cells carried on average 10 mutations, and about 15% of sequences were unmutated. In contrast, nearly all *IGHV* genes of CD27+IgA+ memory-B cells were mutated and contained on average 19 mutations (Fig. 3C) (25). Especially IgA1 transcripts showed a large difference in SHM levels between the two subsets (data not shown) (40). Despite difference in SHM levels, mutations were normally targeted to hypermutable motifs, and appeared to be properly selected during immune responses as reflected by a high ratio of replacement over silent mutations (R/S ratio) of ≥3.2 in their complementarity determining regions (CDR) (Supplemental Fig.1A, 1B; Supplemental Table III).

The Igκ repertoire did not differ between the two IgA+ memory-B-cell subsets and showed predominant *IGKV1* and *IGKV3* subgroup and *IGKJ1* and *IGKJ4* gene usage. Still, CD27−IgA+ memory-B cells showed increased Igλ usage (Supplemental Table II) (25, 41), and differed in the Igλ repertoire from CD27+IgA+ B cells (Fig. 4A) (30). While almost 90% of *IGL* rearrangements in CD27+IgA+ cells involved the *IGLV1* or *IGLV2* subgroups, the rearrangements in CD27−IgA+ B cells reflected the pattern of mature naive-B cells with 29% *IGLV3* and 29% *IGLV2* subgroup usage (Fig. 4B) (42, 43). The increased *IGLV3* usage in CD27−IgA+ B cells was mainly caused by abundant *IGLV3-1* gene (20% vs 0% in CD27+IgA+ cells (Fig. 4C). Further analysis of ~550 *IGLV3* rearrangements bulk-amplified from 7 additional donors revealed that *IGLV3-1* usage within *IGLV3* genes was similar between CD27+IgA+ and CD27−IgA+ B cells (Fig. 5). Thus, the observed increase in single-cell sorted CD27−IgA+ B cells may parallel the overall increase in *IGLV3* usage by these B cells (Fig. 4B). In addition, CD27−IgA+ B cells showed less usage of *IGLJ1* than CD27+IgA+ B cells (17% vs 38%) (Fig. 4B).

Similar to *IGHV*, CD27−IgA+ B cells carried significantly less SHM in the expressed *IGKV* and *IGLV* genes than CD27+IgA+ B cells (Fig. 4D), with slightly more mutations in *IGLV* than *IGKV* in CD27+IgA+ memory-B cells. Analogous to *IGHV*, CD27+IgA+ and CD27−IgA+ B cells showed similar selection of SHM in their *IGKV* and *IGLV* genes with high CDR R/S ratios ranging from 2.8 to 3.4 (data not shown), and positive selection for replacement mutations (Supplemental Fig. 1B, 1C). Interestingly, the *IGLV3-1* genes contained significantly less mutations than other *IGLV3* genes (Fig. 4D, Fig. 5B). These mutations in *IGLV3-1* showed particularly strong selection against replacement mutations in framework regions (FR), while selection in CDR was comparable between *IGLV3-1* and other *IGLV3* genes (Fig. 5C). Hence, the decreased mutation loads in *IGH*, *IGK* and *IGL* combined with the increased Igλ usage in CD27−IgA+ B cells suggest that these B cells were generated towards specific antigens through selection mechanisms that appear distinct from those shaping CD27+IgA+ B cells.

CD27−IgA+ B cells express antibodies with distinct self-reactive features

To determine whether the Ig repertoire differences between CD27+IgA+ and CD27−IgA+ memory-B cells reflect distinct antibody reactivity, we cloned and expressed the amplified Ig heavy and light chain genes as recombinant antibodies. Although not all Ig genes could be expressed *in vitro*, the repertoire of successfully produced recombinant antibodies was representative of the total set with regards to their Ig gene usage, SHM frequency and selection, and IgH-CDR3 characteristics. We tested antibody self-reactivity by immunofluorescence and ELISA against the human Larynx carcinoma cell line HEp-2. We found that CD27+IgA+ B cells expressed significantly more HEp-2 reactive antibodies than their CD27−IgA+ counterparts, representing 35% and 26% of the clones, respectively ($p<0.01$; Fig. 6, A to B). In CD27−IgA+ B cells, the autoreactive antibodies more frequently utilized *IGHV1*, but otherwise these did not differ from non-autoreactive antibodies regarding SHM numbers or IgH-CDR3 length and amino acid composition (data not shown). Autoreactive CD27+IgA+, but not CD27−IgA+ B cells, showed limited selection for replacement mutations in CDRs (Supplemental Fig. 1C, 1D). Immunofluorescence analyses revealed that 11.4% (10/88) of CD27+IgA+ memory-B cells and only 5.3% (4/75) of CD27−IgA+ memory-B cells reacted with cytoplasmic and/or nuclear antigens (Fig. 6, C to D). In addition, CD27−IgA+ B cells were virtually devoid of anti-nuclear clones whereas these represent 4% of CD27+IgA+ B cells (Fig. 6C, 6D). Thus, CD27−IgA+ memory-B cells express antibodies with decreased reactivity against cellular antigens than those produced by CD27+IgA+ B cells.

To determine the multi-specificity of recombinant antibodies, we assessed the frequencies of polyreactive clones that recognized three structurally distinct antigens: double-stranded DNA (dsDNA), insulin and lipopolysaccharide (LPS) (30). We found that CD27−IgA+ B cells contained significantly more polyreactive clones which averaged 26% compared to 16% in CD27+IgA+ memory-B cells (Fig. 7). Polyreactive antibodies often utilized members of the *IGHV1* subgroup, mainly at the expense of *IGHV4* (Fig. 7C). The presence of positively charged amino acids in IgH-CDR3 was not different between polyreactive and non-polyreactive clones, whereas polyreactive antibodies were significantly enriched in very long IgH-CDR3s (≥20 amino acids) (9% in polyreactive vs 1% in non-polyreactive cells;

Fig. 7D). Interestingly, polyreactive antibodies from CD27−IgA+ B cells harbored more *IGHV* SHM than to non-polyreactive CD27−IgA+ clones, at a level similar to that of CD27+IgA+ memory-B cells (Fig. 7E). However, selection of SHM was similar between polyreactive and non-polyreactive clones (Supplemental Fig.1C, 1D; Supplemental Table III).

We conclude that CD27+IgA+ and CD27−IgA+ B cells express antibodies with different self-reactive features; while CD27+IgA+ are enriched in autoreactive clones recognizing cellular components, CD27−IgA+ B cells often produce polyreactive antibodies rarely crossreactive with self and displaying a distinct Ig repertoire associated with increased SHM compared to their non-polyreactive counterparts.

Polyreactive antibodies from IgA+ memory-B cells display anti-bacteria reactivity

Since IgA+ B cells are assumed to produce antibodies protecting mucosa, we tested the reactivity of recombinant antibodies expressed by CD27+IgA+ and CD27−IgA+ memory-B cells with specific microorganisms including commensal bacteria *Bacteroides fragilis, Enterobacter cloacae* and *Enterococcus faecalis*, potentially pathogenic *Clostridium difficile, Escherichia coli* and *Streptococcus aureus*, as well as bacterial flagellin. Irrespective of the tested antigens, the frequencies of reactive antibodies were higher in CD27−IgA+ than in CD27+IgA+ memory-B cells (Fig. 8A). CD27−IgA+ cells showed high binding frequencies for commensal *B. fragilis* and *E. faecalis* strains as well as potentially pathogenic *E. coli* and *C. difficile*, and slightly lower frequency of antibodies binding to *S.aureus* and *E.cloacae*. The frequencies of bacteria-reactive antibodies were consistently higher in CD27−IgA+ B cells than in CD27+IgA+ cells for all 6 analyzed stains (Fig. 8B). Furthermore, nearly all of the strongly bacteria-reactive antibodies were polyreactive (Fig. 8C). Thus, polyreactive antibodies enriched in CD27−IgA+ B cells recognize mucosa-associated bacteria.

Discussion

We reported herein the molecular characterization of unconventional CD27−IgA+ B cells, which share a common gene expression profile with conventional CD27+IgA+ and IgG+ memory-B cells although they express a unique Ig repertoire favoring anti-commensal reactivity.

Despite their postulated origin from TI immune responses, CD27−IgA+ memory-B cells displayed a gene expression profile typical of other memory-B cells. All memory subsets differed from naive-B cells regarding the upregulation of co-stimulatory molecules, downregulation of BCR-signaling inhibitors and naive-B cell-specific transcription factors (34). These changes are thought to underlie the increased B-cell responsiveness of memory-B cells, crucial for adaptive immunity (34). In addition, the increased expression of *IL6R* and *IL10R* shared among memory-B-cell subsets will promote the synergistic effects of IL-6 and IL-10 to induce terminal B-cell differentiation into plasma cells (44–46). *RUNX2* was expressed exclusively by IgA+ B cells, and its expression level was significantly higher (2.4 fold) in CD27−IgA+ than in CD27+IgA+ B cells. *RUNX2* acts downstream of the TGF-β and RA signaling pathways to induce TI class-switching towards IgA in the gut and promote

the terminal differentiation of IgA+ B cells into plasma cells (19, 20, 35). Hence, the restricted *RUNX2* expression identified in IgA+ memory-B cells further support this scenario presiding to their generation. CCR9 mediates homing to the gut, and *CCR9* transcripts were specifically expressed in CD27−IgA+ B cells and it was detected on the cell surface of some of these cells (14). Given the function of CCR9 to direct B-cell migration towards mucous membranes (38, 39, 47), it is possible that protein expression is downregulated in circulating CD27−IgA+ B cells to allow their trafficking to other mucosal locations (48, 49). Altogether, our data indicate that human memory-B-cell subsets share a common genetic program, RUNX2 and CCR9 better define CD27−IgA+ memory-B cells and likely play an important role in mucosal immunity.

We further analyzed the IgH and light chain gene repertoires, and confirmed that CD27−IgA + B cells more frequently expressed Igλ than CD27+IgA+ B cells, and carry significantly fewer SHM in their Ig (25). This could be a direct consequence of a TI origin associated with limited expression of AID (50). However, not all IgA functions in the gut may require extensive affinity maturation (51). It has been postulated that long co-evolution between host and microbiome may favor the selection of Ig variable genes that in germline configuration could recognize conserved bacterial antigens (52). Multiple studies have shown that unmutated IgA isolated from mice colonized with a single bacterial strain can bind antigens with good affinity (3, 53). The distinct Igλ repertoire expressed by CD27−IgA + B cells associated with their increased anti-commensal reactivity may also support this hypothesis. Indeed, *IGLV3-1* genes from CD27−IgA+ memory-B cells carried very few SHM and showed a very strong selection against replacement mutations in FRs. The abundance of *IGLV3-1* has been previously described in diverse tissue-related conditions such as amyloidosis (54). Thus, differences in the *IGL* repertoire of CD27−IgA+ B cells may reflect their involvement in local mucosal responses.

The increased usage of Igλ light chains in the intestinal tract has been proposed to result from ongoing receptor revision processes (41, 55). Our sequence analyses suggest otherwise for the following reasons; first CD27−IgA+ B cells are enriched in *IGLV3-1* genes, which are located downstream of the Igλ locus (41), and in our study contained non-templated nucleotides, reflecting activity of the TdT enzyme. Because TdT is mainly expressed in B-cell progenitors we conclude that Igλ gene rearrangements in CD27−IgA+ memory-B cells were generated during early B-cell development in the bone marrow. Hence, the increased frequencies of Igλ light chains in CD27−IgA+ B cells are most likely the result of selection processes rather than receptor revision.

Differences in Ig repertoire between CD27−IgA+ and CD27+IgA+ B-cell subsets were associated with differences in antibody reactivity. Since all of the studied antibodies were expressed as IgG, we only took into account their antigen-specificity and affinity as mediated by the variable region, and not avidity and effector functions associated with the constant regions. Previous studies reported that human CD27+IgG+ B cells displayed an increased frequency of autoreactive (47%) clones compared to mature naive-B cells (20%) (56, 57). Similarly, we found that CD27+IgA+ B cells also expressed a higher frequency of HEp-2 reactive clones (35%). In contrast, CD27−IgA+ B cells contained less autoreactive clones (26%) and were therefore more similar to mature naive-B cells (30). The lower

frequency of autoreactive antibodies in the CD27−IgA+ subset as compared to CD27+IgA+ and CD27+IgG+ memory-B cells may be explained by their low SHM levels. Autoreactivity in CD27+IgG+ memory-B cells was shown to result from the introduction of SHM (56). Although autoreactive and non-autoreactive CD27−IgA+ had similarly mutated Ig genes, reduced AID activity induced by TI responses in these B cells might provide a basis for the generation of less autoreactive antibodies than in conventional memory-B cells.

The frequency of polyreactive antibodies expressed by CD27−IgA+ B cells was significantly higher than in CD27+IgA+ B cells and comparable with those previously observed for intestinal IgA+ and IgG+ plasmablasts (21). This high antibody polyreactivity may be beneficial for responses towards gastrointestinal bacteria because polyreactive antibodies generated from a specific immune response could serve as ‘natural antibodies’ that recognize other bacterial strains, even upon a first encounter. Interestingly, polyreactive anti-bacteria clones in CD27−IgA+ B cells display higher SHM frequencies than non-polyreactive CD27−IgA+ counterparts, further supporting the importance of SHM in the generation of specific immunity. The role of SHM in the introduction of polyreactivity has also been observed in several studies in mice and human, which demonstrated that reversion of mutated Ig genes to their germline counterparts results in a significant decrease in polyreactivity (42, 56). Moreover, mice carrying a mutated form of AID that allows CSR but not SHM, display severe intestinal lymphoid hyperplasia accompanied by overwhelming microbial expansion in the mucosa (4). Thus, the production of mutated and antigen-selected though polyreactive antibodies by CD27−IgA+ B cells may play an important role in controlling intestinal microbiota in humans.

In summary, we showed that CD27+IgA+ and CD27−IgA+ memory-B-cell subsets contain highly similar transcription profiles, despite their postulated origin from TD and TI immune responses, respectively. However, the distinct antibody repertoire and reactivity of these IgA + memory-B-cell subsets reflects their unique physiological functions with CD27−IgA+ B cells being likely involved in the maintenance of gut homeostasis through the production of polyreactive mutated IgA antibodies with crossreactive anti-bacterial reactivity.

Supplementary Material

Refer to Web version on PubMed Central for supplementary material.

Acknowledgements

We thank Dr. L. Devine, C. Wang and S.J.W. Bartol for cell sorting.

References

1. Arumugam M, Raes J, Pelletier E, Le Paslier D, Yamada T, Mende DR, Fernandes GR, Tap J, Bruls T, Batto JM, Bertalan M, Borruel N, Casellas F, Fernandez L, Gautier L, Hansen T, Hattori M, Hayashi T, Kleerebezem M, Kurokawa K, Leclerc M, Levenez F, Manichanh C, Nielsen HB, Nielsen T, Pons N, Poulain J, Qin J, Sicheritz-Ponten T, Tims S, Torrents D, Ugarte E, Zoetendal EG, Wang J, Guarner F, Pedersen O, de Vos WM, Brunak S, Dore J, Meta HITC, Antolin M, Artiguenave F, Blottiere HM, Almeida M, Brechot C, Cara C, Chervaux C, Cultrone A, Delorme C, Denariaz G, Dervyn R, Foerstner KU, Friss C, van de Guchte M, Guedon E, Haimet F, Huber W, van Hylckama-Vlieg J, Jamet A, Juste C, Kaci G, Knol J, Lakhdari O, Layec S, Le Roux K, Maguin

E, Merieux A, Melo Minardi R, M'Rini C, Muller J, Oozeer R, Parkhill J, Renault P, Rescigno M, Sanchez N, Sunagawa S, Torrejon A, Turner K, Vandemeulebrouck G, Varela E, Winogradsky Y, Zeller G, Weissenbach J, Ehrlich SD, Bork P. Enterotypes of the human gut microbiome. Nature. 2011; 473:174. [PubMed: 21508958]

2. van der Waaij LA, Limburg PC, Mesander G, van der Waaij D. In vivo IgA coating of anaerobic bacteria in human faeces. Gut. 1996; 38:348. [PubMed: 8675085]
3. Hapfelmeier S, Lawson MA, Slack E, Kirundi JK, Stoel M, Heikenwalder M, Cahenzli J, Velykoredko Y, Balmer ML, Endt K, Geuking MB, Curtiss R 3rd, McCoy KD, Macpherson AJ. Reversible microbial colonization of germ-free mice reveals the dynamics of IgA immune responses. Science. 2010; 328:1705. [PubMed: 20576892]
4. Wei M, Shinkura R, Doi Y, Maruya M, Fagarasan S, Honjo T. Mice carrying a knock-in mutation of Aicda resulting in a defect in somatic hypermutation have impaired gut homeostasis and compromised mucosal defense. Nat Immunol. 2011; 12:264. [PubMed: 21258321]
5. Macpherson AJ, McCoy KD, Johansen FE, Brandtzaeg P. The immune geography of IgA induction and function. Mucosal Immunol. 2008; 1:11. [PubMed: 19079156]
6. Ghia P, ten Boekel E, Sanz E, de la Hera A, Rolink A, Melchers F. Ordering of human bone marrow B lymphocyte precursors by single-cell polymerase chain reaction analyses of the rearrangement status of the immunoglobulin H and L chain gene loci. J Exp Med. 1996; 184:2217. [PubMed: 8976177]
7. van Zelm MC, van der Burg M, de Ridder D, Barendregt BH, de Haas EF, Reinders MJ, Lankester AC, Revesz T, Staal FJ, van Dongen JJ. Ig gene rearrangement steps are initiated in early human precursor B cell subsets and correlate with specific transcription factor expression. J Immunol. 2005; 175:5912. [PubMed: 16237084]
8. Cerutti A. The regulation of IgA class switching. Nat Rev Immunol. 2008; 8:421. [PubMed: 18483500]
9. Muramatsu M, Kinoshita K, Fagarasan S, Yamada S, Shinkai Y, Honjo T. Class switch recombination and hypermutation require activation-induced cytidine deaminase (AID), a potential RNA editing enzyme. Cell. 2000; 102:553. [PubMed: 11007474]
10. Fagarasan S, Kinoshita K, Muramatsu M, Ikuta K, Honjo T. In situ class switching and differentiation to IgA-producing cells in the gut lamina propria. Nature. 2001; 413:639. [PubMed: 11675788]
11. Fagarasan S, Honjo T. T-Independent immune response: new aspects of B cell biology. Science. 2000; 290:89. [PubMed: 11021805]
12. Chorny A, Puga I, Cerutti A. Innate signaling networks in mucosal IgA class switching. Adv Immunol. 2010; 107:31. [PubMed: 21034970]
13. Macpherson AJ, Gatto D, Sainsbury E, Harriman GR, Hengartner H, Zinkernagel RM. A primitive T cell-independent mechanism of intestinal mucosal IgA responses to commensal bacteria. Science. 2000; 288:2222. [PubMed: 10864873]
14. Mora JR, Iwata M, Eksteen B, Song SY, Junt T, Senman B, Otipoby KL, Yokota A, Takeuchi H, Ricciardi-Castagnoli P, Rajewsky K, Adams DH, von Andrian UH. Generation of gut-homing IgA-secreting B cells by intestinal dendritic cells. Science. 2006; 314:1157. [PubMed: 17110582]
15. He B, Santamaria R, Xu W, Cols M, Chen K, Puga I, Shan M, Xiong H, Bussel JB, Chiu A, Puel A, Reichenbach J, Marodi L, Doffinger R, Vasconcelos J, Issekutz A, Krause J, Davies G, Li X, Grimbacher B, Plebani A, Meffre E, Picard C, Cunningham-Rundles C, Casanova JL, Cerutti A. The transmembrane activator TACI triggers immunoglobulin class switching by activating B cells through the adaptor MyD88. Nat Immunol. 2010; 11:836. [PubMed: 20676093]
16. Castigli E, Scott S, Dedeoglu F, Bryce P, Jabara H, Bhan AK, Mizoguchi E, Geha RS. Impaired IgA class switching in APRIL-deficient mice. Proc Natl Acad Sci U S A. 2004; 101:3903. [PubMed: 14988498]
17. Castigli E, Wilson SA, Scott S, Dedeoglu F, Xu S, Lam KP, Bram RJ, Jabara H, Geha RS. TACI and BAFF-R mediate isotype switching in B cells. J Exp Med. 2005; 201:35. [PubMed: 15630136]
18. Litinskiy MB, Nardelli B, Hilbert DM, He B, Schaffer A, Casali P, Cerutti A. DCs induce CD40-independent immunoglobulin class switching through BLyS and APRIL. Nat Immunol. 2002; 3:822. [PubMed: 12154359]

19. Borsutzky S, Cazac BB, Roes J, Guzman CA. TGF-beta receptor signaling is critical for mucosal IgA responses. J Immunol. 2004; 173:3305. [PubMed: 15322193]
20. Tokuyama H, Tokuyama Y. Endogenous cytokine expression profiles in retinoic acid-induced IgA production by LPS-stimulated murine splenocytes. Cell Immunol. 1995; 166:247. [PubMed: 7497526]
21. Benckert J, Schmolka N, Kreschel C, Zoller MJ, Sturm A, Wiedenmann B, Wardemann H. The majority of intestinal IgA+ and IgG+ plasmablasts in the human gut are antigen-specific. J Clin Invest. 2011; 121:1946. [PubMed: 21490392]
22. Macpherson AJ, Hunziker L, McCoy K, Lamarre A. IgA responses in the intestinal mucosa against pathogenic and non-pathogenic microorganisms. Microbes Infect. 2001; 3:1021. [PubMed: 11580989]
23. Bollinger RR, Everett ML, Wahl SD, Lee YH, Orndorff PE, Parker W. Secretory IgA and mucin-mediated biofilm formation by environmental strains of Escherichia coli: role of type 1 pili. Mol Immunol. 2006; 43:378. [PubMed: 16310051]
24. Slack E, Hapfelmeier S, Stecher B, Velykoredko Y, Stoel M, Lawson MA, Geuking MB, Beutler B, Tedder TF, Hardt WD, Bercik P, Verdu EF, McCoy KD, Macpherson AJ. Innate and adaptive immunity cooperate flexibly to maintain host-microbiota mutualism. Science. 2009; 325:617. [PubMed: 19644121]
25. Berkowska MA, Driessen GJ, Bikos V, Grosserichter-Wagener C, Stamatopoulos K, Cerutti A, He B, Biermann K, Lange JF, van der Burg M, van Dongen JJ, van Zelm MC. Human memory B cells originate from three distinct germinal center-dependent and -independent maturation pathways. Blood. 2011; 118:2150. [PubMed: 21690558]
26. Kett K, Brandtzaeg P, Radl J, Haaijman JJ. Different subclass distribution of IgA-producing cells in human lymphoid organs and various secretory tissues. J Immunol. 1986; 136:3631. [PubMed: 3517160]
27. Berkowska MA, Grosserichter-Wagener C, Adriaansen HJ, de Ridder D, Mirani-Oostdijk KP, Agteresch HJ, Bottcher S, Orfao A, van Dongen JJ, van Zelm MC. Persistent polyclonal B-cell lymphocytosis: extensively proliferated CD27+IgM+IgD+ memory B cells with a distinctive immunophenotype. Leukemia. 2014; 28:1560. [PubMed: 24549258]
28. Nodland SE, Berkowska MA, Bajer AA, Shah N, de Ridder D, van Dongen JJ, LeBien TW, van Zelm MC. IL-7R expression and IL-7 signaling confer a distinct phenotype on developing human B-lineage cells. Blood. 2011; 118:2116. [PubMed: 21680796]
29. Ludbrook J. Multiple comparison procedures updated. Clin Exp Pharmacol Physiol. 1998; 25:1032. [PubMed: 9888002]
30. Wardemann H, Yurasov S, Schaefer A, Young JW, Meffre E, Nussenzweig MC. Predominant autoantibody production by early human B cell precursors. Science. 2003; 301:1374. [PubMed: 12920303]
31. Meffre E, Schaefer A, Wardemann H, Wilson P, Davis E, Nussenzweig MC. Surrogate light chain expressing human peripheral B cells produce self-reactive antibodies. J Exp Med. 2004; 199:145. [PubMed: 14699083]
32. Tiller T, Meffre E, Yurasov S, Tsuiji M, Nussenzweig MC, Wardemann H. Efficient generation of monoclonal antibodies from single human B cells by single cell RT-PCR and expression vector cloning. J Immunol Methods. 2008; 329:112. [PubMed: 17996249]
33. Hershberg U, Uduman M, Shlomchik MJ, Kleinstein SH. Improved methods for detecting selection by mutation analysis of Ig V region sequences. Int Immunol. 2008; 20:683. [PubMed: 18397909]
34. Good KL, Avery DT, Tangye SG. Resting human memory B cells are intrinsically programmed for enhanced survival and responsiveness to diverse stimuli compared to naive B cells. J Immunol. 2009; 182:890. [PubMed: 19124732]
35. Watanabe K, Sugai M, Nambu Y, Osato M, Hayashi T, Kawaguchi M, Komori T, Ito Y, Shimizu A. Requirement for Runx proteins in IgA class switching acting downstream of TGF-beta 1 and retinoic acid signaling. J Immunol. 2010; 184:2785. [PubMed: 20142360]
36. Warnock RA, Askari S, Butcher EC, von Andrian UH. Molecular mechanisms of lymphocyte homing to peripheral lymph nodes. J Exp Med. 1998; 187:205. [PubMed: 9432978]

37. Bargatze RF, Jutila MA, Butcher EC. Distinct roles of L-selectin and integrins alpha 4 beta 7 and LFA-1 in lymphocyte homing to Peyer's patch-HEV in situ: the multistep model confirmed and refined. Immunity. 1995; 3:99. [PubMed: 7542550]
38. Kunkel EJ, Kim CH, Lazarus NH, Vierra MA, Soler D, Bowman EP, Butcher EC. CCR10 expression is a common feature of circulating and mucosal epithelial tissue IgA Ab-secreting cells. J Clin Invest. 2003; 111:1001. [PubMed: 12671049]
39. Pabst O, Ohl L, Wendland M, Wurbel MA, Kremmer E, Malissen B, Forster R. Chemokine receptor CCR9 contributes to the localization of plasma cells to the small intestine. J Exp Med. 2004; 199:411. [PubMed: 14744993]
40. Wu YC, Kipling D, Dunn-Walters DK. The relationship between CD27 negative and positive B cell populations in human peripheral blood. Front Immunol. 2011; 2:81. [PubMed: 22566870]
41. Su W, Gordon JN, Barone F, Boursier L, Turnbull W, Mendis S, Dunn-Walters DK, Spencer J. Lambda light chain revision in the human intestinal IgA response. J Immunol. 2008; 181:1264. [PubMed: 18606680]
42. Tsuiji M, Yurasov S, Velinzon K, Thomas S, Nussenzweig MC, Wardemann H. A checkpoint for autoreactivity in human IgM+ memory B cell development. J Exp Med. 2006; 203:393. [PubMed: 16446381]
43. Yurasov S, Wardemann H, Hammersen J, Tsuiji M, Meffre E, Pascual V, Nussenzweig MC. Defective B cell tolerance checkpoints in systemic lupus erythematosus. J Exp Med. 2005; 201:703. [PubMed: 15738055]
44. Zhang Y, Lin JX, Vilcek J. Synthesis of interleukin 6 (interferon-beta 2/B cell stimulatory factor 2) in human fibroblasts is triggered by an increase in intracellular cyclic AMP. J Biol Chem. 1988; 263:6177. [PubMed: 2452159]
45. Burdin N, Rousset F, Banchereau J. B-cell-derived IL-10: production and function. Methods. 1997; 11:98. [PubMed: 8990095]
46. Defrance T, Vanbervliet B, Briere F, Durand I, Rousset F, Banchereau J. Interleukin 10 and transforming growth factor beta cooperate to induce anti-CD40-activated naive human B cells to secrete immunoglobulin A. J Exp Med. 1992; 175:671. [PubMed: 1371300]
47. Hieshima K, Kawasaki Y, Hanamoto H, Nakayama T, Nagakubo D, Kanamaru A, Yoshie O. CC chemokine ligands 25 and 28 play essential roles in intestinal extravasation of IgA antibody-secreting cells. J Immunol. 2004; 173:3668. [PubMed: 15356112]
48. Holtmeier W, Hennemann A, Caspary WF. IgA and IgM V(H) repertoires in human colon: evidence for clonally expanded B cells that are widely disseminated. Gastroenterology. 2000; 119:1253. [PubMed: 11054383]
49. Dunn-Walters DK, Boursier L, Spencer J. Hypermutation, diversity and dissemination of human intestinal lamina propria plasma cells. Eur J Immunol. 1997; 27:2959. [PubMed: 9394824]
50. He B, Xu W, Cerutti A. Comment on "Gut-associated lymphoid tissue contains the molecular machinery to support T-cell-dependent and T-cell-independent class switch recombination". Mucosal Immunol. 3:92. [PubMed: 20016479]
51. Stoel M, Jiang HQ, van Diemen CC, Bun JC, Dammers PM, Thurnheer MC, Kroese FG, Cebra JJ, Bos NA. Restricted IgA repertoire in both B-1 and B-2 cell-derived gut plasmablasts. J Immunol. 2005; 174:1046. [PubMed: 15634929]
52. Slack E, Balmer ML, Fritz JH, Hapfelmeier S. Functional flexibility of intestinal IgA - broadening the fine line. Front Immunol. 2012; 3:100. [PubMed: 22563329]
53. Bos NA, Bun JC, Popma SH, Cebra ER, Deenen GJ, van der Cammen MJ, Kroese FG, Cebra JJ. Monoclonal immunoglobulin A derived from peritoneal B cells is encoded by both germ line and somatically mutated VH genes and is reactive with commensal bacteria. Infect Immun. 1996; 64:616. [PubMed: 8550216]
54. Perfetti V, Casarini S, Palladini G, Vignarelli MC, Klersy C, Diegoli M, Ascari E, Merlini G. Analysis of V(lambda)-J(lambda) expression in plasma cells from primary (AL) amyloidosis and normal bone marrow identifies 3r (lambdaIII) as a new amyloid-associated germline gene segment. Blood. 2002; 100:948. [PubMed: 12130507]

55. Su W, Boursier L, Padala A, Sanderson JD, Spencer J. Biases in Ig lambda light chain rearrangements in human intestinal plasma cells. J Immunol. 2004; 172:2360. [PubMed: 14764705]

56. Tiller T, Tsuiji M, Yurasov S, Velinzon K, Nussenzweig MC, Wardemann H. Autoreactivity in human IgG+ memory B cells. Immunity. 2007; 26:205. [PubMed: 17306569]

57. Scheid JF, Mouquet H, Kofer J, Yurasov S, Nussenzweig MC, Wardemann H. Differential regulation of self-reactivity discriminates between IgG+ human circulating memory B cells and bone marrow plasma cells. Proc Natl Acad Sci U S A. 2011; 108:18044. [PubMed: 22025722]

Abbreviations

SHM	somatic hypermutations
CSR	class-switch recombination
CDR	complementarity determining region
FR	framework region
AID	activation-induced cytidine deaminase
TD	T-cell dependent
TI	T-cell independent
TLR	Toll-like receptor
DC	dendritic cell
RA	retinoic acid

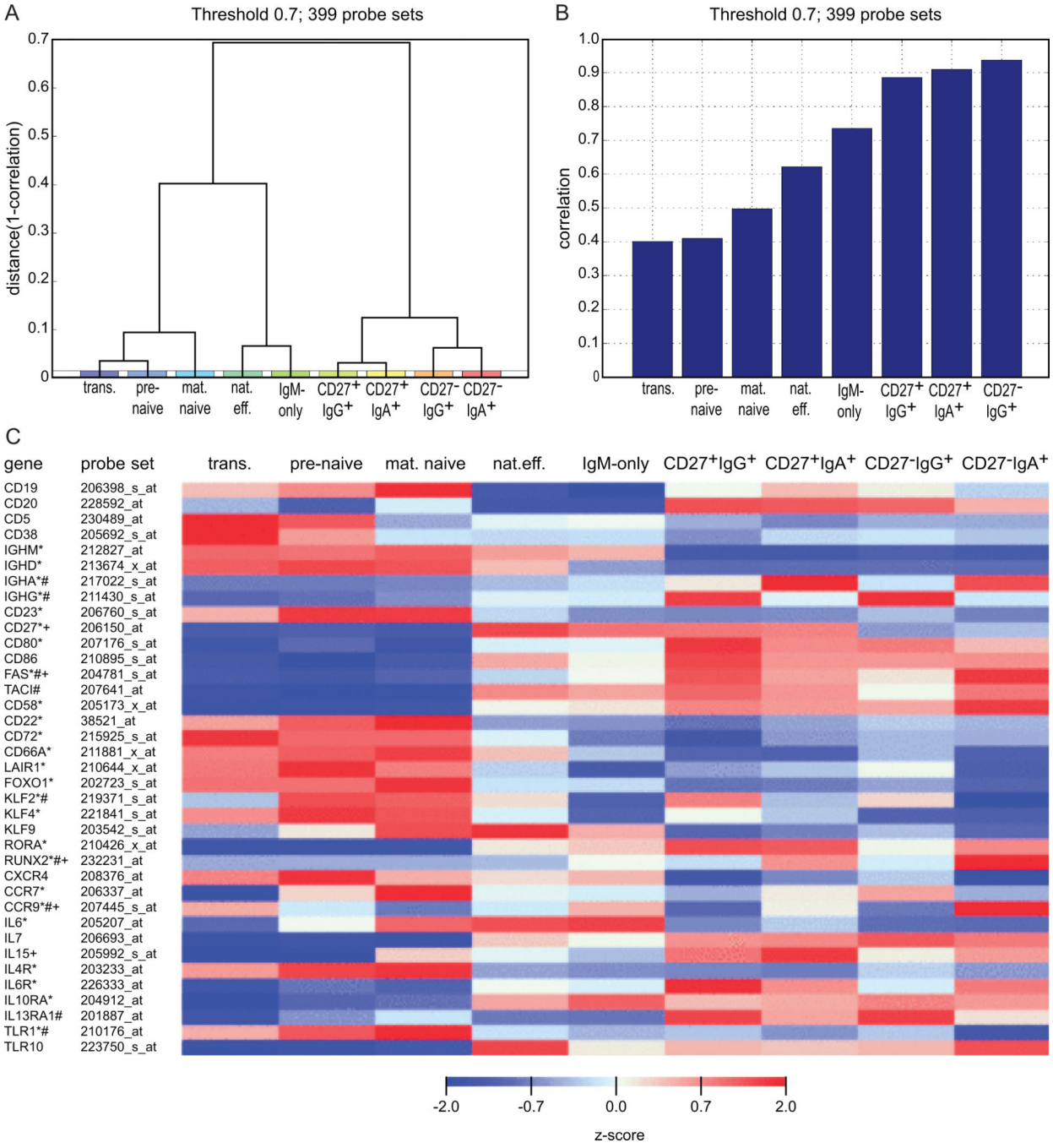

FIGURE 1.

Gene expression profiling of naive and memory-B-cell subsets. (**A**) Hierarchical clustering (complete linkage) using 1-correlation as a distance measure based on the 399 probe sets that showed the most variation between any two samples (threshold at $\log_2$ value 0.7). Clustering analyses was performed without bias for known genes or subsets. (**B**) Correlation of the gene expression profiles of these 399 genes for CD27−IgA+ memory-B cells as compared to the naive and memory-B-cell subsets. (**C**) Heat map with normalized expression levels of selected probe sets in naive and memory-B-cell subsets. Z-scores were

maximized to −2 and 2. *, statistically significant difference between CD27+IgA+ and mature naive-B cells; #, statistically significant difference between CD27−IgA+ and mature naive-B cells; +, statistically significant difference between CD27+IgA+ and CD27−IgA+ B cells

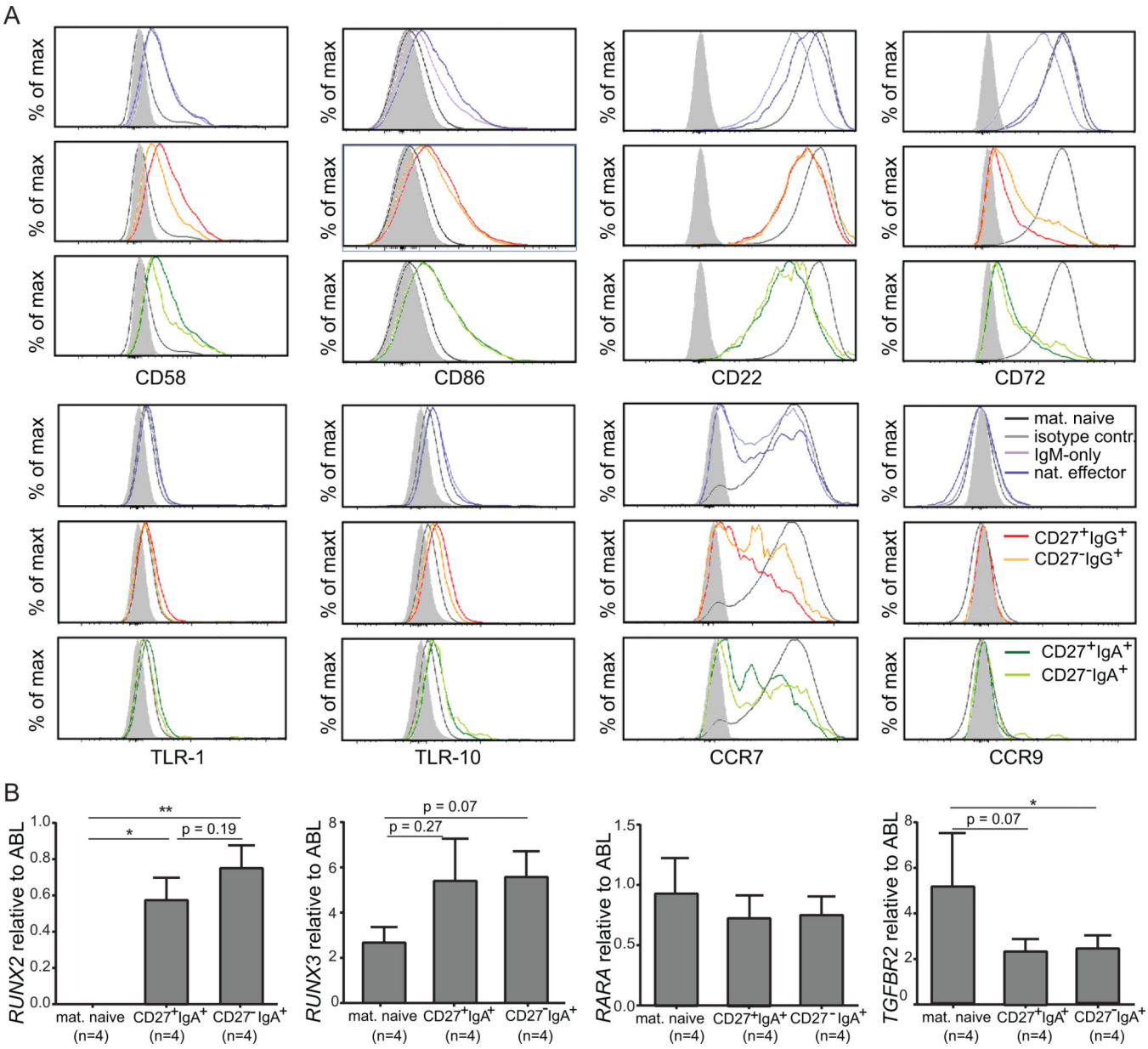

FIGURE 2.

Expression levels of selected markers on memory-B-cell subsets. **(A)** Expression levels of selected co-stimulatory molecules (CD58, CD86), BCR-signaling inhibitors (CD22, CD72), Toll-like receptors (TLR-6, TLR-10) and chemokine receptors (CCR7, CCR9) were analyzed by flow cytometry on IgM+, IgG+ and IgA+ memory-B-cell subsets. Each plot contains a light grey filled histogram representing the isotype control, and a dark grey histogram representing mature naive-B cells. **(B)** Expression levels of selected genes were analyzed by RQ-PCR. Each bar represents a mean fold expression relative to control gene ABL with SEM error bars. The number of analyzed samples is indicated between brackets below the name of the subset.

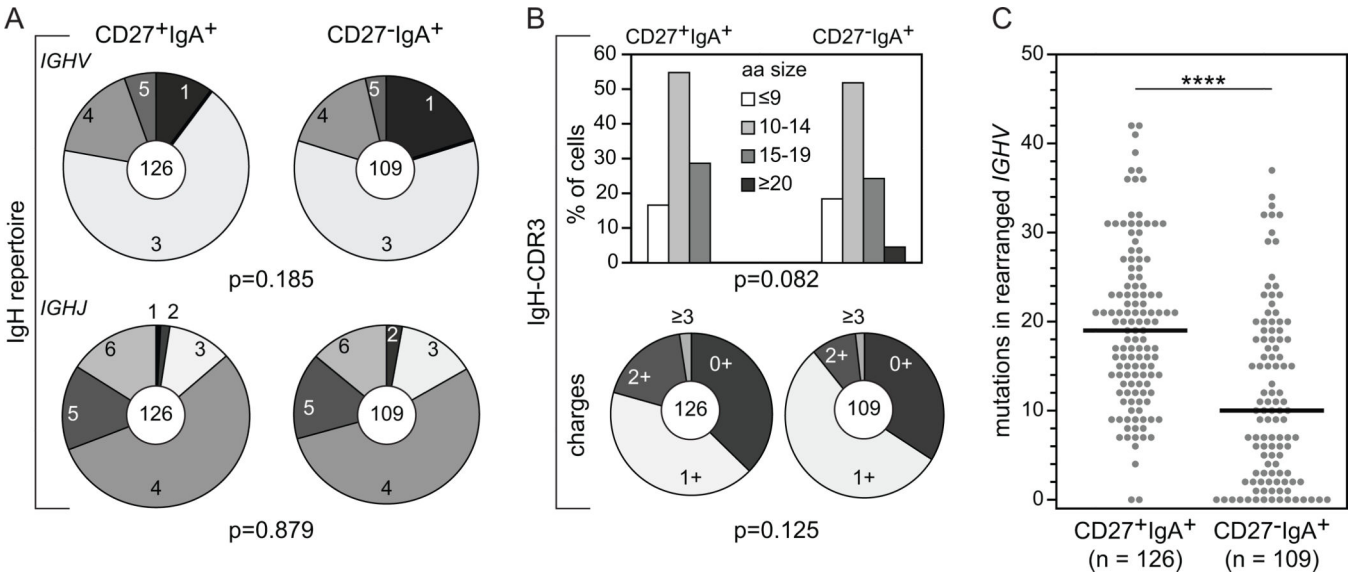

FIGURE 3.

IgH gene repertoire and characteristics in CD27+IgA+ and CD27−IgA+ memory-B cells. (**A**) *IGHV* subgroup (upper panel) and *IGHJ* gene (lower panel) usage in IgA+ B-cell subsets. The numbers of analyzed sequences are indicated in the inner circles. (**B**) IgH-CDR3 length (upper panel) and charge (lower panel) distributions. (**C**) The number of SHM in rearranged *IGHV* genes. Each grey dot represents an individual sequence and black lines represent median values. Statistical analysis of the data was performed with the $\chi 2$ test in (**A**) and (**B**) and with the Mann-Whitney test in (**C**); ****, $p<0.0001$

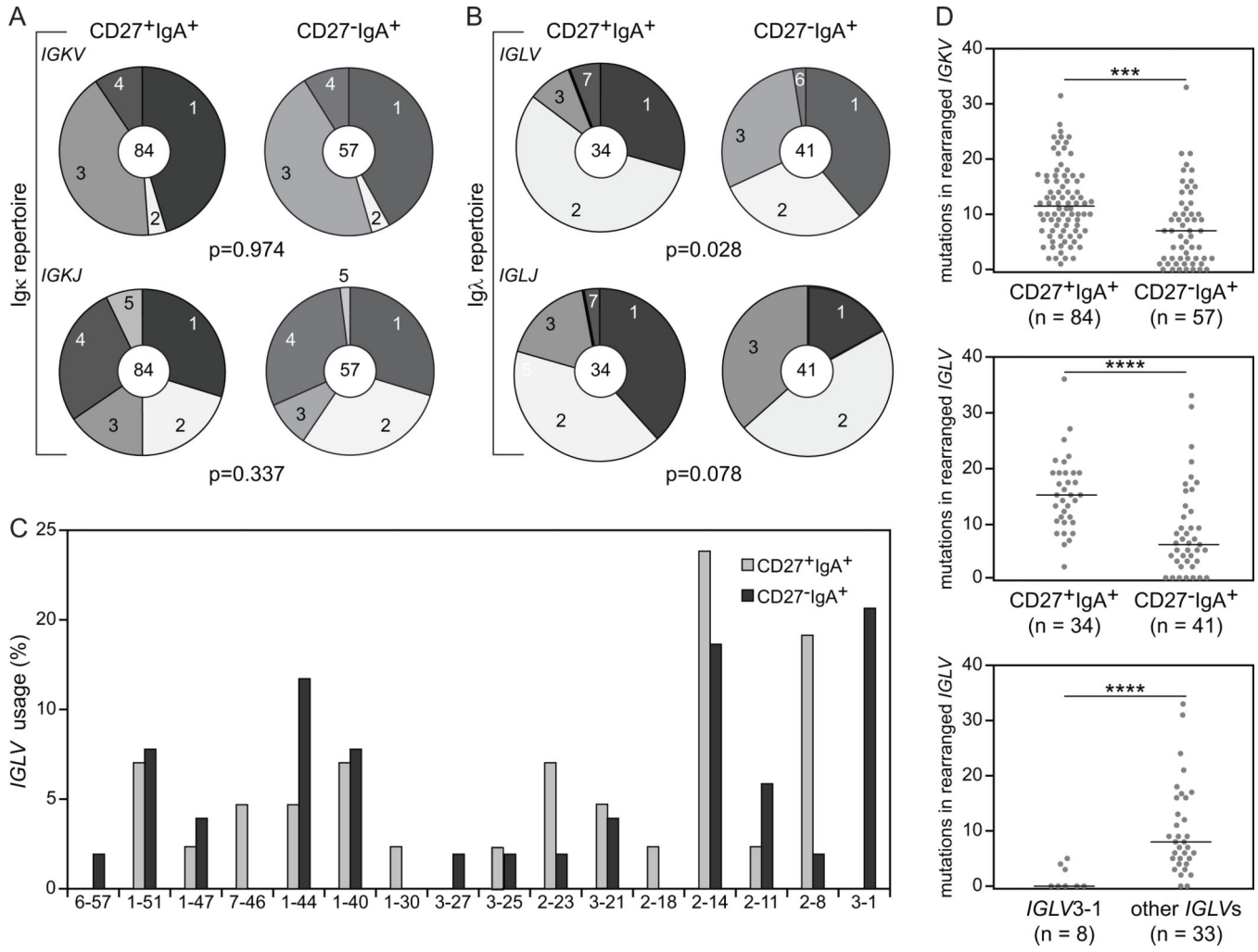

FIGURE 4.

Igκ and Igλ light chain gene repertoire and characteristics in CD27+IgA+ and CD27−IgA+ memory-B cells. (**A**) *IGKV* subgroup (upper panel) and *IGKJ* gene (lower panel) use in IgA + memory-B-cell subsets. The numbers of analyzed sequences are indicated in the inner circles. (**B**) *IGLV* subgroup (upper panel) and *IGLJ* gene (lower panel) use. (**C**) *IGLV* gene use. (**D**) The number of SHM in rearranged *IGKV* (upper panel) and *IGLV* (middle panel) in memory-B-cell subsets, and in *IGLV3-1* and non-*IGLV3-1* genes of CD27−IgA+ memory-B cells (bottom panel). Each grey dot represents an individual sequence and black lines represent median values. Statistical analysis of the data was performed with the $\chi 2$ test in (**A**) and (**B**), and with the Mann-Whitney test in (D); ***, $p<0.001$; ****, $p<0.0001$

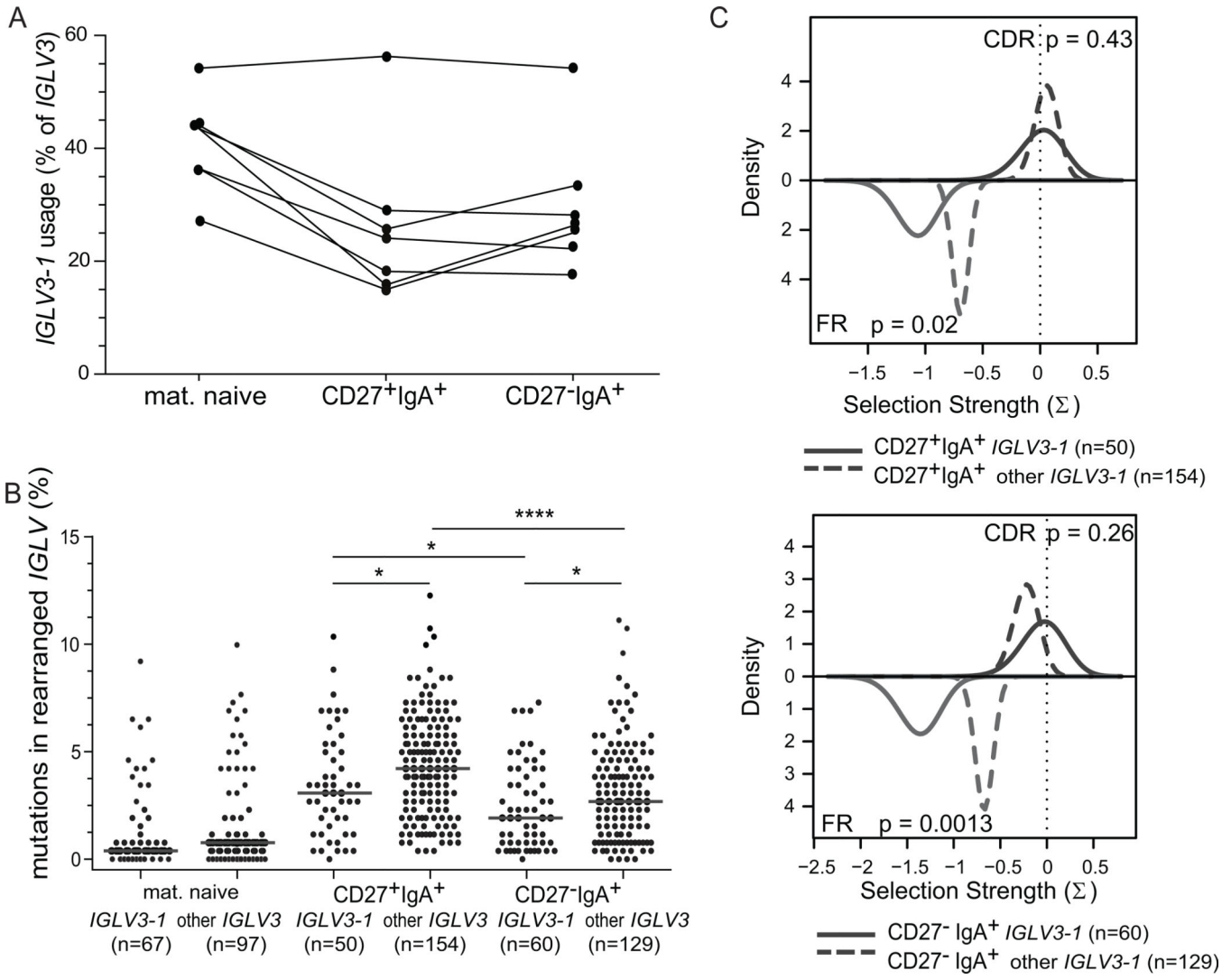

FIGURE 5.

Usage and characteristics of *IGLV3-1* gene. (**A**) Frequency of *IGLV3-1* gene in *IGLV3* subgroup in mature naive, CD27+IgA+ and CD27−IgA+ B cells from 7 independent donors. *IGL* rearrangements were amplified with forward *IGLV3*-specific and two reverse *IGLJ1* and IGLJ2/3-specific primers. In total 557 unique productive rearrangements were analyzed. (**B**) Frequency of SHM in rearranged *IGLV3-1* and non-*IGLV3-1* genes in mature naive, CD27+IgA+ and CD27−IgA+ memory-B cells from 7 donors. Each grey dot represents an individual sequence and black lines represent median values. Data was statistically analyzed with the Mann-Whitney test. *, p<0.05; ****, p<0.0001. (**C**) Selection of SHM in *IGLV3-1* and other *IGLV3* genes in CD27+IgA+ B cells (top panel) and CD27−IgA+ B cells (bottom panel), as measured with the BASELINe program (https://selection.med.yale.edu/baseline). In both panels, red lines represent CDRs, blue lines represent FRs.

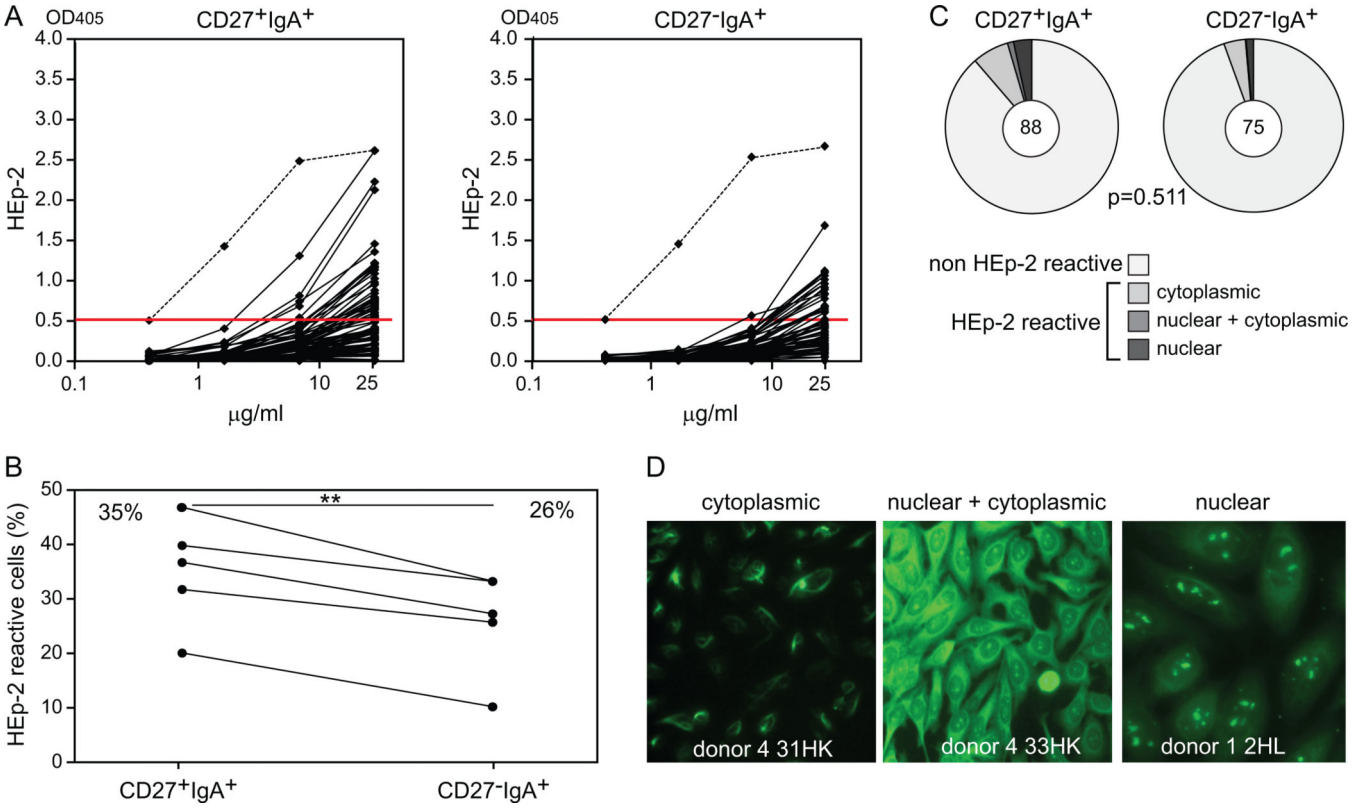

FIGURE 6.

Autoreactivity in CD27+IgA+ and CD27−IgA+ memory-B-cell subsets. (**A**) Reactivity to HEp-2 cell lysates of 88 antibodies from CD27+IgA+ cells and 75 antibodies from CD27−IgA+ cells derived from 5 healthy donors. The dashed line represents the highly reactive ED45 positive control (31), and the red line represents a cut-off value of 0.5 above which antibodies were considered as HEp-2 reactive. (**B**) Frequencies of HEp-2 reactive CD27+IgA+ and CD27−IgA+ cells in 5 donors. Data points representing values for the same donor are connected with a black line. Statistical analysis was performed with the two-tailed Student's *t* test for paired samples; **, $p<0.01$ (**C**) Autoreactivity patterns of CD27+IgA+ and CD27−IgA+ cells as measured in an immunofluorescence assay (IFA) with HEp-2 cell–coated slides. The numbers of analyzed antibodies are indicated in the inner circles. Statistical analysis of the data was performed with the $\chi 2$ test. (**D**) Representative pictures from IFA staining; original magnification, 40×.

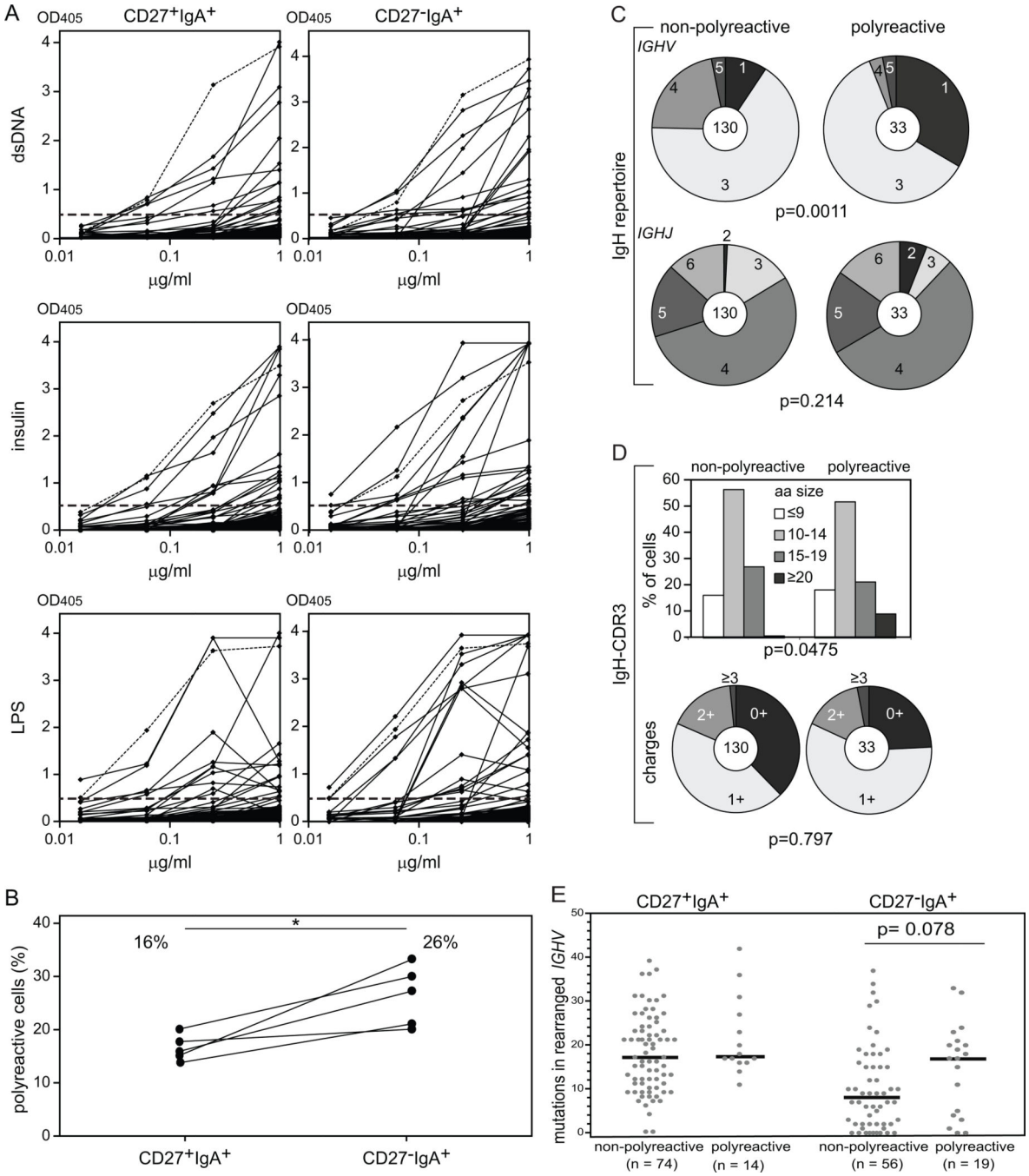

FIGURE 7.

Polyreactivity in CD27+IgA+ and CD27−IgA+ memory-B-cell subsets. (**A**) Antibodies showing triple-reactive against dsDNA (upper panel), insulin (middle panel), and LPS (lower panel) were defined as polyreactive. In total, 88 antibodies from CD27+IgA+ and 75 antibodies from CD27−IgA+ memory B cells were analyzed. Dashed lines represent the highly reactive ED45 positive control (31). (**B**) Frequencies of polyreactive CD27+IgA+ and CD27−IgA+ antibodies in 5 donors. Data points representing values for one donor are connected with a black line. (**C**) *IGHV* subgroup (upper panel) and *IGHJ* gene (lower panel)

use in polyreactive and non-polyreactive IgA+ memory-B cells. The numbers of analyzed sequences are indicated in the inner circles. (**D**) IgH-CDR3 length (upper panel) and charge (lower panel) distributions. (**E**) The numbers of SHM in rearranged *IGHV* genes. Each grey dot represents an individual sequence and black lines represent median values. Statistical analysis was performed with the two-tailed Student's *t* test for paired samples in (**B**), with the $\chi 2$ test in (**C**) and (**D**) and with the Mann-Whitney test in (E); *, $p<0.05$

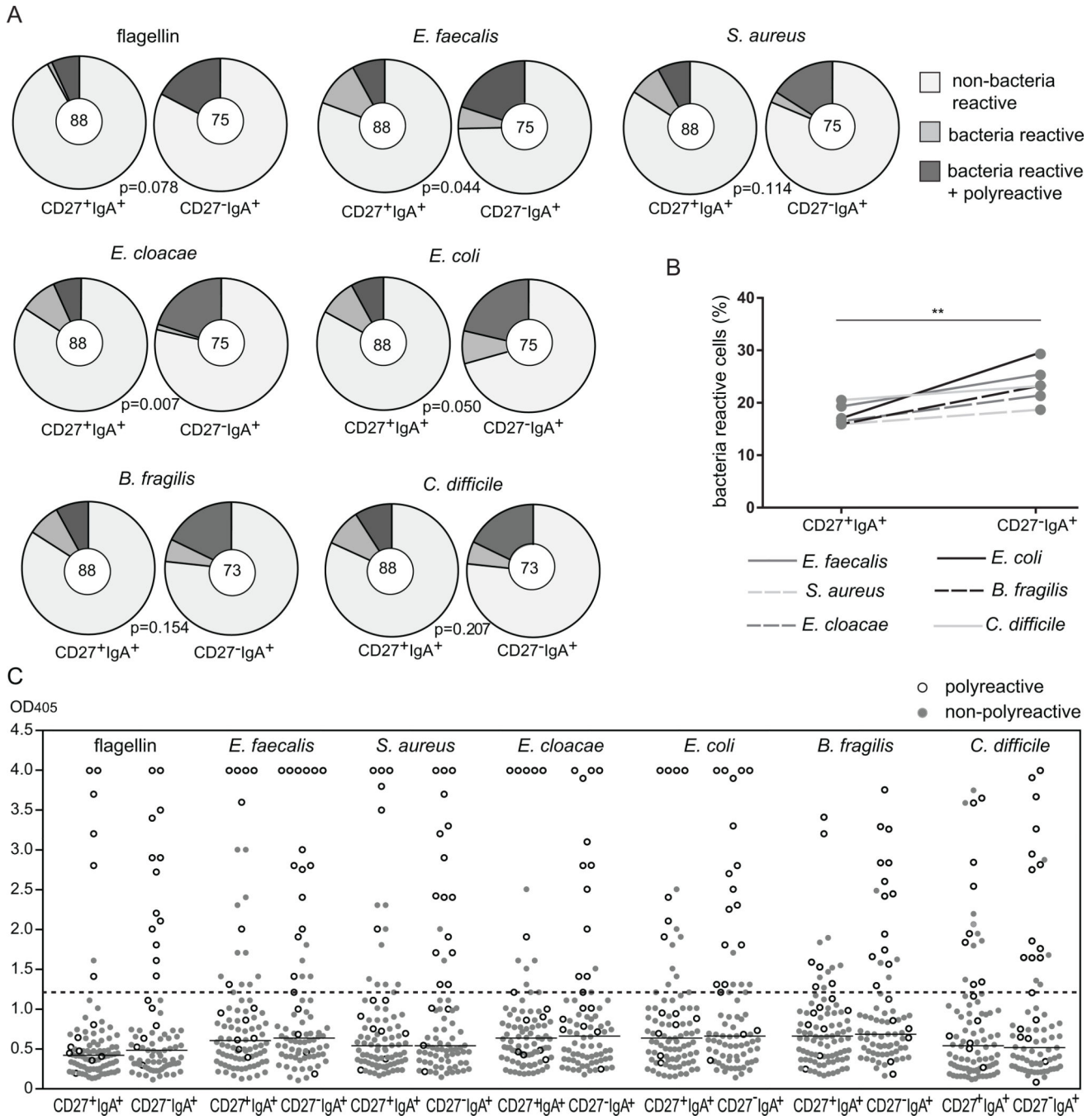

FIGURE 8.

Reactivity of CD27+IgA+ and CD27−IgA+ memory-B cells with commensal and potentially pathogenic bacteria. (**A**) Pie charts summarizing the frequencies of antibodies from CD27+IgA+ and CD27−IgA+ memory-B cells with reactivities against flagellin, commensal bacteria (*B. fragilis*, *E. cloacae*, *E. faecalis*) and potentially pathogenic bacteria (*E. coli*, *S. aureus*, *C.difficile*). The numbers of analyzed antibodies are indicated in the inner circles. (**B**) Overall bacteria reactivities of CD27+IgA+ and CD27−IgA+ memory-B cells. (**C**) Reactivity levels against bacteria as measured by ELISA for antibodies from CD27+IgA

+ and CD27−IgA+ memory-B cells. Each grey dot represents a non-polyreactive antibody, and each white dot a polyreactive antibody. Black lines represent median values of all antibodies together, and a dashed line represents a threshold value above which antibodies were considered bacteria reactive. In (**A**) data was statistically analyzed with the $\chi 2$ test. In (**B**) was performed with the two-tailed Student's *t* test for paired samples; **, $p<0.01$